



Research & Reviews On

Electrochemistry

Full Paper

RREC, 5(3), 2014 [51-59]

Fabrication and Microhardness properties of SiC and Gr reinforced Ni-based nanocomposite thin film

Abbas Fahami*, Bahman Nasiri-Tabrizi

Materials Engineering Department, Najafabad Branch, Islamic Azad University, Najafabad, Isfahan, (IRAN)

E-mail : ab.fahami@gmail.com

ABSTRACT

Nickel based nanocomposite thin films were prepared from a Watts type electrolyte containing reinforcement's particles (SiC and Gr) to deposit on steel St-37 substrate. The effect of different bath temperatures was investigated to optimize high quality coatings. The experimental outcomes were characterized by X-ray diffraction (XRD), scanning electron microscopy (SEM), energy dispersive X-ray spectroscopy (EDS), Elemental mapping analysis system, field emission scanning electron microscopy (FE-SEM), and Micro hardness tester. Based on XRD results, the main peaks in the samples were nickel, nickel oxide and SiC phases. Microscopic observations illustrated a cluster like structure which consisted of some fine sphere particles with an average particle size of about 65 nm. Results revealed that optimum bath parameters were the temperature of 45 (°C). The hardness of the coatings was also measured and found to be 412 to 543 (Hv) depending on the bath parameters and the reinforcements weight percentage (wt.%) in the Ni matrix. Ultimately, the results demonstrated that the electrochemical parameter had considerable influences on the morphology and mechanical properties of the Ni-SiC-Gr coatings.

© 2014 Trade Science Inc. - INDIA

KEYWORDS

Electrochemical parameters;
Ni-SiC-Gr;
Microhardness;
Morphological features.

INTRODUCTION

Recently, promotion of low carbon steel (St-37) surface was evaluated by numerous investigators so that researches and developments on nickel matrix composite coatings have come into prominence which can meet the industrial request^[1-4]. It was proved that the uniform dispersion of the co-deposited particles such as Ni, Pd, Cu, Ni-P, Ni-W and Ni-Fe-Cr leads to the improvement of mechanical and the tribological properties of parts surface^[5,6]. For coatings preparation,

several methods such as electrodeposition, ion implantation, chemical vapor deposition (CVD), laser beam deposition, physical vapor deposition (PVD), plasma and high-velocity oxygen fuel (HVOF) spraying have been served^[7,8]. The electrochemical deposition of nano-size ceramic particles in a metallic matrix has led to a new generation of composites due to the advantages of this technique. The easy maintainability, easy low working temperatures, low cost and high production rate are the remarkable features of this method^[9].

In chemical techniques, the optimum bath param-

Full Paper

eters have been used to absorb the fine particles on the surface. In this approach, the repulsion force between particles with the same charges can be increased. This, in turn, reduces the agglomeration and provides a solution with more stable particles. The use of nano-size particles in coatings could be declined the problem of created imperfection such as voids between the particles and matrix interfaces. In addition, the deposition of enough amounts of reinforced particles could lead to generation of stronger and more resistant covers. Also, electrodeposition as an appropriate procedure was proposed to facilitate deposition of fine particulates onto the low carbon steel surface. Nickel matrix coatings have received widespread acceptance as it provides a uniform deposit on irregular surfaces, direct deposition on surface activated, high hardness and excellent resistance to wear, abrasion and corrosion. Additionally, nickel as an engineering material was broadly used among the electrodeposited surfaces^[10]. Several studies were demonstrated that deposition of coatings in the presence of fine particles such as a hard materials (ceramics particles) or lubricating particles (PTFE and graphite (Gr)) into the nickel matrix, might effectively improve the mechanical and tribological properties of the surfaces^[11-21]. Research on electrodeposition of nanocomposite coatings has been directed towards the determination of optimum conditions for their production, i.e. bath temperature, pH value, stirring speed, current density and particles concentration in electrolyte. Meanwhile, by manipulating the processing parameters some remarkable results were acquired^[22]. It should be noted that the choosing of optimum circumstances for production of nickel coatings from the reported results is difficult because they are, in some cases, different or paradoxical^[23].

The plating parameters are very effective in electrochemical deposition of Ni-based coatings in order to promote morphological and mechanical properties of nickel (Ni) matrix coating with addition of reinforcement particles (silicon carbide (SiC) and graphite (Gr)); therefore obtaining of precise determination of these parameters was the main target of this paper. Also, the influence of electrochemical parameters on the morphological and mechanical characteristics of Ni-SiC-Gr nanocomposite coatings on the St-37 substrate was investigated. In addition, a comparison study of the properties of these coatings at different conditions was conducted. For this aim, the optimum states of the plating parameter such as bath temperature ($^{\circ}\text{C}$) was evaluated by X-ray diffraction (XRD), field emission scanning electron microscopy (FE-SEM), scanning electron microscopy (SEM), energy dispersive X-ray spectroscopy (EDS), and Elemental mapping analysis. In addition, the microhardness of specimens was measured by Micro hardness Tester, so that the outcomes showed remarkable consequences.

EXPERIMENTAL PROCEDURES

Nickel- based nanocomposite coating preparation

Ni- based coatings were deposited from Watts bath by direct current (DC) electroplating. The basic components of the electrolyte were consisted of nickel sulfate (Merck, 99%), boric acid (Merck, 99.8%) and nickel chloride (Merck, 98%). The plating compositions and the experimental operating parameters are shown in TABLE 1. Silicon Carbide (Hefeikaier Nanometer Energy & Technology, 99%) in the range of 40 – 100 nm and graphite (Merck, 99.8%) micro particle range of 5 – 100 μm were used in the experiments

TABLE 1 : Overview of electrochemical plating conditions

Bath composition (g/l)		Operating conditions	
NiSO ₄ .6H ₂ O	200	Temperature (T $^{\circ}\text{C}$)	45-55-65-75
NiCl ₂ .6H ₂ O	20	pH	4.8
H ₃ BO ₃	40	Current density (A/ dm ²)	4
SiC	12	Stirring speed (rpm)	500
Graphite	1	Plating time (min)	20
CTAB	5	Electrolyte volume (cc)	100
SDS	5	Anode	Ni
C ₇ H ₅ NO ₃ S	1	Cathode	St-37

as the reinforcing phases, respectively. The surfactants such as cetyltrimethylammonium bromide (CTAB, Merck 98%), sodiumdodecyl sulfate (SDS, Acros Organics 98%) and Saccharine (Merck 99%) were utilized to increase the electrostatic adsorption of suspended particles on the cathode surface by enhancement of their positive charge^[25]. In order to investigate the effect of bath temperatures, four temperatures (45, 55, 65, and 75 °C) were applied. The plating conditions were a current density of 4 A/dm², a pH of 4.8, a rpm of 500, and 12 g/l SiC particle contents in electrolyte. The electrochemical plating of all the specimens was performed for 20 min by magnetite stirring for each electroplating run. Furthermore, the sonication process time was 15 min to provide homogeneous dispersion and to prevent agglomeration of the particles.

Low carbon steel (St-37) plates with dimensions of 10 mm × 10 mm × 1 mm were used as the substrate (cathode) and also nickel cylindrical was utilized as a anode for electroplating process. In brief, the preparation of the specimen's surfaces was carried out at three stages; degreasing, acid pickling and polishing. After each step, the plates have been rinsed by distilled water to remove the residuals of each stage, completely.

Characterization of electrodeposited Ni matrix nanocomposite coatings

Phase analyses and structural changes of deposited layers were determined by X-ray diffraction (Philips X-ray diffractometer (XRD), $Cu-K_{\alpha}$ radiation, 40 kV, 30 mA and 0.02 ° S⁻¹ step scan). For qualitative analysis, XRD graphs were recorded in the interval $20^{\circ} \leq 2\theta \leq 70^{\circ}$ at scan speed of 1°/min. This range covers two strongest peaks of nickel and also two peaks of SiC. "PANalytical X'Pert HighScore" software was also utilized for the analysis of different peaks. The gained patterns were compared to standards compiled by the Joint Committee on Powder Diffraction and Standards (JCPDS), which involved card #04-0850 for Ni, #029-1128 for SiC and #047-1049 for NiO. The morphologies of coatings surfaces were observed by scanning electron microscopy (SEM, VEGA Tescan easyprobe). X-ray energy dispersion spectroscopy (EDS) and Elemental mapping analysis system which were coupled with SEM were utilized to determine the weight percentage of nanoparticles and distribution of particles

(voltage used for EDX equal to 20 kV). The weight percentages of particles were measured at three different locations at same magnification of the images. The mean values are reported along with positive and negative error bars. A field emission scanning electron microscope (FE-SEM Hitachi S1831) that operated at the acceleration voltage of 15 kV was served to measure the particulates size and thickness of the thin layers. For this purpose, the plate's surfaces were coated with gold for more electronic conduction. A Vickers micro-hardness tester (MICROMET3, Buehler Ltd.USA) with Vickers pyramidal diamond indenter was served to analyze microhardness of the layers polished at room temperature. A load of 50 (g) was performed for 20 s and the final value quoted for the hardness of the deposit was the average of at least three measurements. It should be noted that the reported values of the microhardness are representative of the deposited coatings without significant influence from underlying substrate.

RESULTS AND DISCUSSIONS

XRD analysis

Figure 1 shows the X-ray diffractions of Ni matrix nanocomposite coatings deposited at different bath temperatures (°C). The profiles of the samples confirm the presence of Ni, SiC, graphite (Gr) and NiO phases and no characteristic peaks of other phases have been recorded. Meanwhile, the presence of NiO as an extra phase demonstrates that the surface of the Ni matrix was oxidized during contacting with the plating bath^[26]. Note that the peaks corresponding to Gr particles could not be completely identified in the XRD patterns from nanocomposite coatings due to very low content (1 g/L). Moreover, the intensity of the Ni peaks at different bath temperatures has been changed so that it can affect the crystallinity of nickel in the matrix. The peak intensities of SiC are also hardly noticeable. All the XRD patterns at different conditions display typical peaks corresponding to (111) and (200) crystallographic planes of nickel as well as the (102) and (110) planes of SiC. It has been reported that the embedding of SiC nano-particles in the nickel matrix could be modified the Ni texture from the soft [1 0 0] mode to the mixed

Full Paper

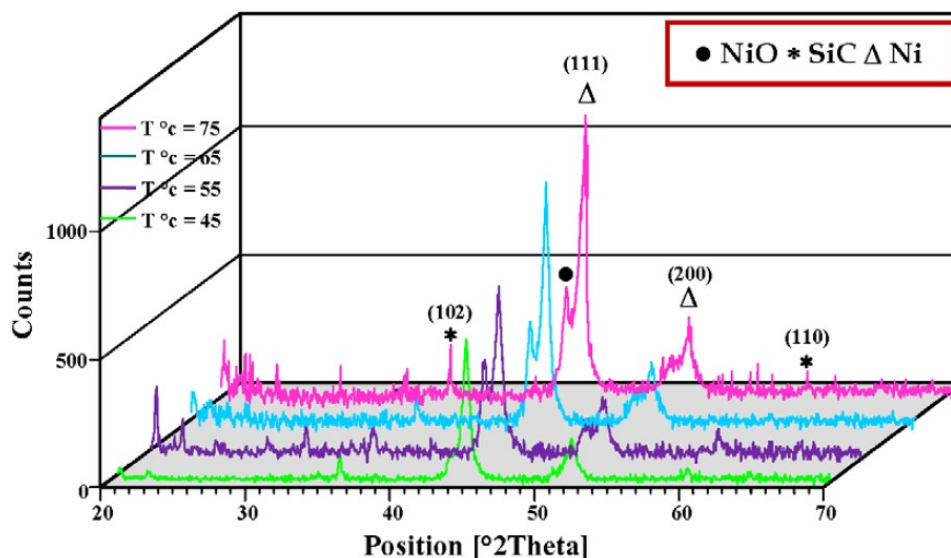


Figure 1 : XRD patterns of Ni–SiC–Gr nanocomposite thin films deposited at different bath temperatures (45, 55, 65, and 75 °C)

preferred [2 1 1] orientation^[27]. For all the deposited coatings at various temperatures, the intensity of the (111) peaks is higher than the other planes. This result indicated that the preferred orientation of Ni is (111) plane. It should be mentioned that the (111) peak at $2\theta = 44.508^\circ$ is the strongest peak (relative intensity = 100 %) in the standard XRD pattern from randomly oriented polycrystalline nickel (No. 04–0850).

The crystallite size (D) for nickel composite coatings was calculated using Scherrer equation^[28]:

$$\text{FWHM} = \frac{K\lambda}{D\cos\theta} \frac{180^\circ}{\pi} \quad (1)$$

Where FWHM is full width half maxima in 2θ degrees, D is the crystallite size in nm, K is constant (usually evaluated as 0.94), and λ is the wavelength of Cu K α radiation (0.154 nm). The crystallinity percentage (CrI) of Ni phase for all the samples was determined by using the XRD data according to the following equation^[29]:

$$\text{CrI} = \frac{I_{111} - I_{\text{am}}}{I_{111}} \times 100 \quad (2)$$

Where I_{111} is the diffraction intensity of (111) plane and I_{am} is the intensity of the measured amorphous peak. Also, as a part of structural characteristics, the influence of bath parameters on Ni lattice (cubic) parameter constant (a_c) was evaluated by the equation^[30]:

$$d_{hkl} = \frac{a_c}{\sqrt{(h^2 + k^2 + l^2)}} \quad (3)$$

Where the Miller indices (hkl) obtained from the diffraction spectra were identified using JCPDS cards (No. 04-0850) and d_{hkl} is the distance between adjacent Bragg planes. TABLE 2 shows the effect of bath temperature on the average crystallite size (D), crystallinity percentage (%) and lattice parameter constant (a_c) of Ni phase in the nanocomposite coatings which were calculated using XRD data. According to data, the crystallite size and crystallinity of nickel increased with rising of bath temperature (45–75 °C). This phenomenon was attributed to the effect of bath temperature on the structural features. Finally, crystallite size and crystallinity of nickel at temperature of 45 °C were 20.3 nm and 84.4 %, respectively. The obtained data shows that by increasing bath temperature from 45 °C to 75 °C, the crystallite size and crystallinity of nickel increases mostly after 45 °C and reaches a maximum at 75 °C of temperature. In fact, increasing the bath temperature might assist grain growth although all the composite coatings were comprised of nano-sized crystallites. It

TABLE 2 : The average crystallite size (D), crystallinity percentage (%), and lattice parameter constant (a_c) of Ni phase as a function of different bath temperatures (45, 55, 65, and 75 °C)

	Bath temperature (T ?c)			
	45	55	65	75
D (nm)	20.3	21.9	23	28.2
CrI (%)	84.4	88.5	91.3	92.7
a_c (Å)	3.526	3.525	3.523	3.519

should be mentioned that the growth of coatings is controlled both by the nucleation and crystal growth rate. In the electrodeposition process, reinforcement's nanoparticles that adhere to the cathode surface act as nucleation sites and hence accelerate nickel matrix nucleation. During the process of electrocrystallization, grain nucleation and crystal growth occur simultaneously and are competitive^[31].

TABLE 2 also displays the lattice parameter (a_c) of nickel as function of bath temperature. From this data, the lattice parameter values for all the samples are close to the standard value (# 04-0850: $a=3.5228 \text{ \AA}$) which indicates that diverse bath temperature have very little effect on the lattice constant of Ni during plating

process.

SEM and FE-SEM observations

Figure 2 shows the surfaces morphology of Ni–SiC–Gr nanocomposite thin film deposited at different bath parameters. As can be seen in Figure 2, a cluster like structure containing of fine grains as well as some agglomerates were deposited on St–37 substrates at different bath temperatures ($^{\circ}\text{C}$). By increasing of bath temperature in the range $45\text{--}75 \text{ }^{\circ}\text{C}$, continuous evolution of the morphological features was appeared.

The mean size of particulates was risen by increasing of electrolyte temperature, so only a slight change in particle size of the sample ($T = 75 \text{ }^{\circ}\text{C}$) was observed.

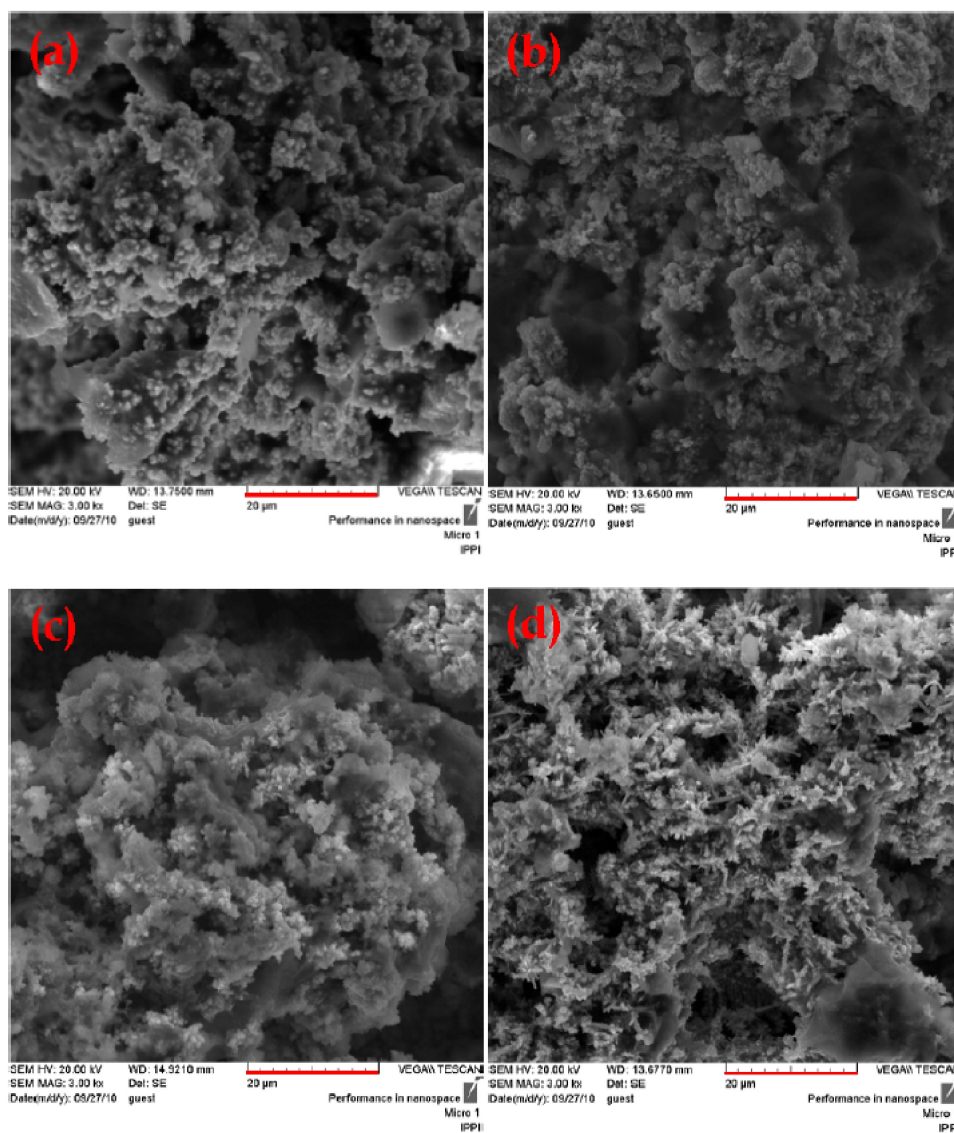


Figure 2 : SEM micrographs of Ni–SiC–Gr nanocomposite coatings deposited at different bath temperatures (45, 55, 65, and $75 \text{ }^{\circ}\text{C}$)

Full Paper

However, the bath evaporation rate also increases as does the energy consumption; therefore, it is better to run at a low temperature as long as the quality of coatings is not affected. In order to compare the coatings, the surface deposited at bath temperature of 45 °C has a homogenous morphology. It seems that other samples are not regular so that there were much more pores at higher temperatures.

The cross-sectional images of Ni–SiC–Gr nanocomposite coatings deposited at various bath parameters is shown in Figure 3. As can be seen, all the coatings deposited at various bath temperatures were almost uniform and homogenous. From higher magnifi-

cation of FE-SEM observations, it is observed that Ni–SiC–Gr nanocomposite coatings were formed as spherical globules with the average crystallite size of 62 nm. It seems that the particles have tendency to adhere on the clean upper surface of the substrate (St–37). The thickness of the coatings prepared at different bath temperatures were decreased by increasing bath temperatures, so that the obtained coating at temperature of 45 °C was interestingly thicker than the other films. While hydrogen evolution at the cathode can also result in coating thickness reduction, such effects are not of electrodeposition from watts bath. Furthermore, boric acid in the electrolyte is known for suppressing the hy-

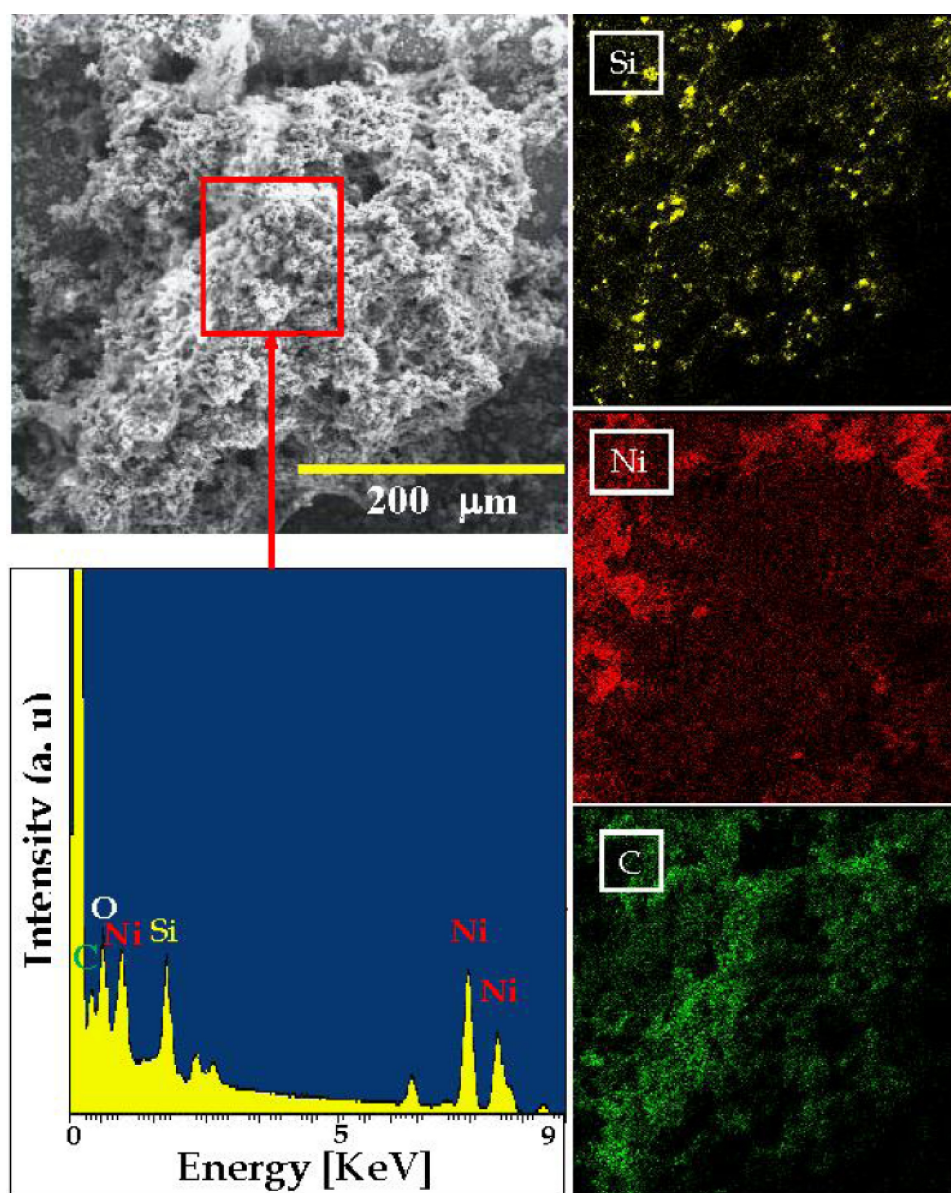


Figure 4 : EDS and Elemental mapping spectra of Ni–SiCGr nanocomposite coatings deposited at optimum bath temperature of 45 °C

drogen evolution during electrodeposition of nickel from watts bath. The result is in agreement with other research^[31].

EDS and Elemental mapping analysis

The EDS (Energy dispersive X-ray spectroscopy) spectra of NiSiC–Gr nanocomposite coating deposited at optimum bath parameters (bath temperature of 45 °C) is shown in Figure 4. The results confirm the presence of Ni, Si, C, and O elements in the nanocomposites. Since, there is no specific separation in this analysis between carbon of graphite and carbide structures, the displayed carbon signals derived from silicon carbide and graphite sources. Furthermore, it is noteworthy to mention that chemically stable contaminants were not detected and also it demonstrates that the Ni–SiC–Gr nanocomposite coatings on the St–37 have relatively acceptable purity. According to Elemental mapping analysis, the distribution of reinforced materials such as SiC and Gr as well as Ni particles are depicted (see Figure 4), the dispersion of particles is uniformly homogenous in the samples. It seems that the attendance of reinforcement's particulates resulted in the changing of surface charges on the substrate and affected the deposition rate^[32]. Therefore, determination of optimal bath parameters of electrochemical plating can develop the efficiency of electrodeposition process of nickel based nanocomposite coatings.

To investigate the influence of reinforcement contents on the microstructure and properties of composite coatings, several Ni–SiC–Gr nanocomposite coatings were deposited by varying bath temperatures (Figure 5). The variation of SiC and Gr contents in the nickel composite coatings as a function of bath temperatures (45, 55, 65, and 75 °C) is shown in Figure 5.

The weight percentage (wt.%) of SiC and Gr in the composite coatings at temperature of 45 °C is relatively more than the other temperatures. Since SiC particles and Gr should be transported to the cathode for the co-deposition, the different temperatures affects the wt.% of SiC and Gr co-deposited a great deal.

Microhardness analysis

The microhardness of coatings as a function of varied bath temperatures is presented in Figure 6. Based on Figure 6, the microhardness of coatings had changed

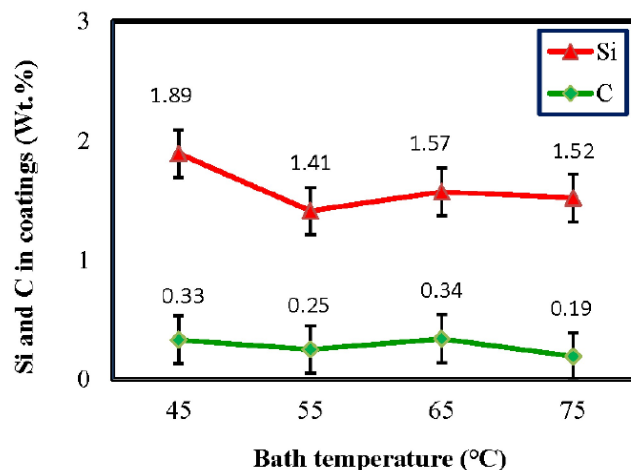


Figure 5 : Reinforcement content in the Ni–SiC–Gr nanocomposite coatings as a function of different bath temperatures (45, 55, 65, and 75 °C)

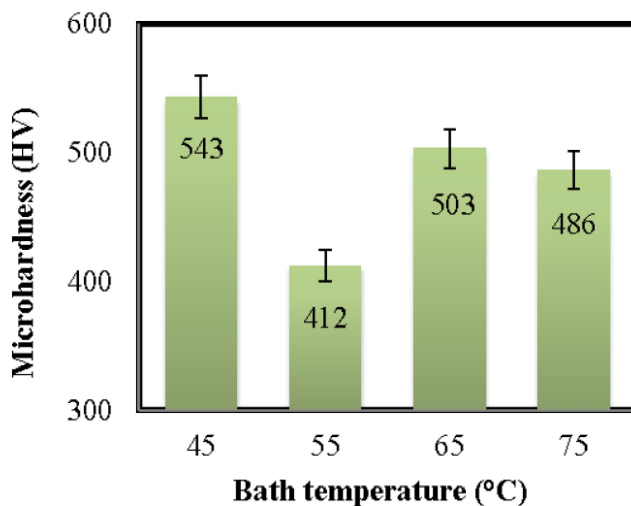


Figure 6 : Variation of microhardness of Ni–SiC–Gr nanocomposite coatings deposited at different bath temperatures (45, 55, 65, and 75 °C)

at diverse bath temperatures (45, 55, 65, and 75 °C). The maximum hardness (543 Hv) is corresponding to the coating deposited at temperature of 45 °C. As discussed earlier, this temperature also resulted in increasing content of reinforce nanoparticles in the coatings. Thus, the improvements in the hardness of nanocomposite coating deposited at 45 °C condition seem to be due to rising content of reinforced particles in the coatings. Furthermore, in the case of higher bath temperatures, the intensive convection of solutions increases the probability of particle collision, so that they cause agglomeration owing to their poor wettability, which decreases the particle content in composite coatings^[33]. It can be seen that the hardness of the coatings

Full Paper

is proportional to the content of reinforced particles in the coatings. It should be mentioned that the SiC particles deposited into Ni matrix are as obstacles versus the growth of the Ni grains and the plastic deformation of the matrix. The results are in good agreement with the microscopic observation and EDS analysis.

CONCLUSION

The effect of electrochemical parameter on the morphological and mechanical features of Ni–SiC–Gr nanocomposite coatings on St–37 substrate was investigated. The effect of diverse bath temperatures (°C) was evaluated to optimize high quality coatings with suitable mechanical and morphological features. The results revealed that the optimum conditions to deposit Ni matrix nanocomposite coatings were the bath temperature of 45 °C. According to the XRD results, the significant peaks in the specimens were nickel and SiC phases which were almost similar in all the coatings deposited at different bath temperatures. Based on SEM and FE-SEM observations, a cluster like structure with an average particle size of about 62 nm was observed. Also, the depositions were controlled to obtain a specific thickness between 40 and 200 μm; thus, the thickness of coating at optimum bath temperature was acquired 116 μm. For all the nanocomposite coatings, the maximum amount of reinforcements (SiC and Gr) in the coatings emerged in the optimal bath circumstances. Eventually, the coating prepared at optimum bath conditions illustrated maximum microhardness about 543 HV which was in accordance with the SEM and EDS results.

ACKNOWLEDGMENT

The authors are grateful to research affairs of Islamic Azad University, Najafabad Branch for supporting this research.

REFERENCES

[1] D.Chaliampalias, G.Vourlias, E.Pavlidou, S.Skolianos, K.Chrissafis, G.Stergioudis; Comparative examination of the microstructure and high temperature oxidation performance of NiCrBSi flame

- sprayed and pack cementation coatings. *Appl.Surf.Sci.*, **255**, 3605-3612 (2009).
- [2] V.Vitry, A.F.Kanta, F.Delaunoi; Application of nitriding to electroless nickel–boron coatings: Chemical and structural effects; mechanical characterization; corrosion resistance. *Mater Des.*, **39**, 269-278 (2012).
- [3] V.Vitry, A.F.Kantab, Delaunoi; Initiation and formation of electroless nickel–boron coatings on mild steel: Effect of substrate roughness. *Mater.Sci.Eng.B.*, **175**, 266-273 (2010).
- [4] B.Ramezanzadeh, M.M.Attar; Studying the corrosion resistance and hydrolytic degradation of an epoxy coating containing ZnO nanoparticles. *Mater Chem Phys*, **130**, 1208-1219 (2011).
- [5] J.X.Kang, W.Z.Zhao, G.F.Zhang; Influence of electrodeposition parameters on the deposition rate and microhardness of nanocrystalline Ni coatings. *Surf.Coat.Technol.*, **203**, 1815-1818 (2009).
- [6] P.Sahoo, S.K.Das; Tribology of electroless nickel coatings – A review. *Materials and Design*, **32**, 1760-1775 (2011).
- [7] S.C.Tjong, H.Chen; Nanocrystalline materials and coatings. *Mater.Sci.Eng.R.*, **45**, 1 (2004).
- [8] C.Suryanarayana, C.C.Koch; Nanocrystalline materials – Current research and future directions. *Hyperfine Interact*, **130**, 5 (2000).
- [9] P.Gyftou, M.Stroumbouli, E.A.Pavlatou, P.Asimidis, N.Spyrellis; Tribological study of Ni matrix composite coatings containing nano and micro SiC particles. *Electrochim.Acta*, **50**, 4544-4550 (2005).
- [10] C.Zanella, M.P.Lekka, L.Bonora; Influence of the particle size on the mechanical and electrochemical behaviour of micro and nano-nickel matrix composite coatings. *J.Appl.Electrochem.*, **39**, 31-38 (2009).
- [11] E.Broszeit; Mechanical, thermal and tribological properties of electro- and chemo deposited composite coatings. *Thin Solid Films*, **95**, 133 (1982).
- [12] I.Garcia, J.Fransaer, J.P.Celis; Electrodeposition and sliding wear resistance of nickel composite coatings containing micron and submicron SiC particles. *Surf.Coat.Technol.*, **148**, 171 (2001).
- [13] M.Surender, B.Basu, R.Balasubramaniam; Wear characterization of electrodeposited Ni–WC composite coatings. *Tribol.Int.*, **37**, 743 (2004).
- [14] V.V.N.Reddy, B.Ramamoorthy, N.P.Kesava; A study on the wear resistance of electroless Ni-P/diamond composite coatings. *Wear*, **239**, 111-116 (2000).

- [15] F.B.Bahaideen, M.R.Zaidi, A.A.Zainal; Electroless Ni-P-C_g (graphite)- SiC composite coating and its application onto piston rings of a small two stroke utility engine. *J.Sci.Ind.Res.*, **69**, 830-834 (2010).
- [16] Y.Wu, B.Shen, L.Liu, W.Hu; The tribological behaviour of electroless Ni-P-Gr-SiC composite. *Wear*, **261**, 201-207 (2006).
- [17] S.K.Kim, H.J.Yoo; Formation of bilayer Ni-SiC composite coatings by electrodeposition. *Surf Coat Technol*, **108**, 564-569 (1998).
- [18] Z.X.Niu, F.H.Cao, W.Wang, Z.Zhang, J.Q.Zhang, C.N.Cao; Electrodeposition of Ni-SiC nanocomposite film. *Trans Nonferrous Met Soc china*, **17**, 9-15 (2007).
- [19] M.D.Ger; Electrochemical deposition of nickel/SiC composites in the presence of surfactants. *Mater Chem Phys*, **87**, 67-74 (2004).
- [20] M.C.Choua, M.D.Ger, S.T.Ke, Y.R.Huangc, S.T.Wu; The Ni-P-SiC composite produced by electro-codeposition. *Mater.Chem.Phys*, **92**, 146-151 (2005).
- [21] A.Hovestad, L.J.J.Janssen; Electrochemical codeposition of inert particles in a metallic matrix, *J.Appl.Electro.chem.*, **25**, 519-527 (1995).
- [22] S.C.Wang, W.C.J.Wei; Kinetics of electroplating process of nano sized ceramic particle/Ni composite. *Mater.Chem.Phys.*, **78**, 574-580 (2003).
- [23] F.Hu, K.C.Chan; Electro codeposition behavior of Ni-SiC composite under different shaped waveforms. *Appl.Surf.Sci.*, **233**, 163-171 (2004).
- [24] R.Elanshezian, B.Ramamoorthy, P.Kesavan Nair; Effect of surfactants on the mechanical properties of electroless (Ni-P) coating. *Surf.Coat.Technol.*, **203**, 709-712 (2008).
- [25] L.Burzynska, E.Rudnik, J.Koza, C.BlazL, W.Szymanski; Electrodeposition and heat treatment of nickel/silicon carbide composites. *Surf.Coat.Technol.*, **202**, 2545-2556 (2008).
- [26] M.R.Vaezi, S.K.Sadrnezhaad, L.Nikzad; Electrodeposition of Ni-SiC nano-composite coatings and evaluation of wear and corrosion resistance and electroplating characteristics. *Colloids Surf.A.*, **315**, 176-182 (2008).
- [27] T.Borkar, S.P.Harimkar; Effect of electrodeposition conditions and reinforcement content on microstructure and tribological properties of nickel composite coatings. *Surf.Coat.Technol.*, **205**, 4124-4134 (2011).
- [28] Z.Liao, Z.Huang, H.Hua, Y.Zhang, Y.Tan; Microscopic structure and properties changes of cassava stillage residue pretreated by mechanical activation. *BioResource.Technol.*, **102**, 7953-7958 (2011).
- [29] M.A.Siddig, S.Radiman, S.V.Muniandy, L.S.Jan; Structure of cubic phases in ternary systems Glucopone/water/hydrocarbon. *Colloids.Surf.A.*, **236**, 57-67 (2004).
- [30] A.M.Rashidi, A.Amadeh; Effect of Electroplating Parameters on Microstructure of Nanocrystalline Nickel Coatings. *J.Mater.Sci.Technol.*, **26**, 82-86 (2010).
- [31] P.Wang, Y.L.Cheng, Z.Zhang; A study on the electrocodeposition processes and properties of Ni-SiC nanocomposite coatings. *J.Coat.Technol.Res.*, **8**, 409-417 (2011).
- [32] H.Gül, F.Kiliç, S.Aslan, A.Alp, H.Akbulut; Characteristics of electro-co-deposited Ni-Al₂O₃ nanoparticle reinforced metal matrix composite (MMC) coatings. *Wear*, **267**, 976-990 (2009).
- [33] Y.N.Gou, W.J.Huang, R.C.Zeng, Y.Zhu; Influence of pH values on electroless Ni-P-SiC plating on AZ91D magnesium alloy. *Trans Nonferrous Met Soc China*, **20**, 674-678 (2010).